JOURNAL OF MOLECULAR SPECTROSCOPY 54, 200–214 (1975)

Millimeter- and Submillimeter-Wave Length Spectrum of the Partially Deuterated Ammonias; A Study of Inversion, Centrifugal Distortion, and Rotation–Inversion Interactions[1]

FRANK C. DE LUCIA AND PAUL HELMINGER[2]

Department of Physics, Duke University, Durham, North Carloina 27706

Eighty-two new rotation–inversion transitions of the light asymmetric rotors NH_2D and ND_2H have been measured in the 80–600 GHz region by means of high resolution microwave techniques. Included among these transitions are several submillimeter *R*-branch transitions which make possible a calculation of both the rotational and distortion parameters which characterize the molecule. An accurate inversion Hamiltonian is developed and used as a preliminary step to a rotation–distortion treatment of the molecule. The spectrum of ND_2H reveals the existence of a rotation–vibration interaction which significantly alters the energy of a number of ground vibrational state levels. The results of an analysis technique which incorporates the effects of this perturbation as well as the inversion effects are presented. This procedure makes possible the analysis of all observed transitions to within experimental uncertainties as well as the accurate prediction of unobserved transitions. The rotational constants which result from this work are (MHz): For NH_2D, O^+ vibrational state, $\mathfrak{A} = 290\,286.53 \pm 0.21$, $\mathfrak{B} = 192\,240.15 \pm 0.42$, $\mathfrak{C} = 140\,602.50 \pm 0.42$; for NH_2D, O^- vibrational state, $\mathfrak{A} = 290\,192.14 \pm 0.21$, $\mathfrak{B} = 192\,176.27 \pm 0.42$, $\mathfrak{C} = 140\,625.64 \pm 0.42$; for ND_2H, O^+ vibrational state, $\mathfrak{A} = 223\,222.92 \pm 0.18$, $\mathfrak{B} = 160\,433.96 \pm 0.17$, $\mathfrak{C} = 112\,305.40 \pm 0.17$; for ND_2H, O^- vibrational state, $\mathfrak{A} = 223\,147.21 \pm 0.14$, $\mathfrak{B} = 160\,423.37 \pm 0.13$, $\mathfrak{C} = 112\,313.72 \pm 0.13$.

INTRODUCTION

Microwave spectroscopists have studied ammonia and its unique rotation–inversion spectrum more extensively than any other molecule. Most of this work has been concentrated on studies of the inversion spectra of NH_3 and ND_3 in the easily accessible centimeter wave region (*1*, *2*). In addition, several rotational transitions of these species as well as of NT_3 have been observed in the millimeter and submillimeter wave regions (*3*, *4*). Although these studies have made significant contributions to the understanding of the ammonia molecule, an accurate and comprehensive analysis of the rotation–inversion spectrum of the partially deuterated ammonias provides new and important information which cannot be obtained from studies of the symmetric forms. Investigations of the pure inversion spectrum of ammonia provide no information on the rotational constants, and while measurements of the rotational spectra of NH_3, ND_3, and NT_3 provide only the value of B, the values of A, B,

[1] This work was supported by the National Science Foundation, Grant GP-34590 and by the U. S. Army Research Office, Grant DA-ARO-D-31-124-72-G96.

[2] Present address: Department of Physics, University of South Alabama, Mobile, Alabama 36688.

and C can all be determined from an analysis of the asymmetric species. Similarly, the distortion parameters of these molecules provide considerable information about the molecular force field which is not contained in the D_J and D_{JK} of the symmetric top forms (*5*).

In addition, both the inversion splittings and the change of the rotational constants with vibrational state are important benchmarks for further development of models of the potential barrier to inversion. Although there has been considerable theoretical investigation of this problem (*6*), it has never been possible to adequately account for the known experimental data. Recently, Papousek, Stone, and Spirko (*7*) have applied the techniques of Hougen, Bunker, and Johns (*8*) to NH_3 and ND_3 and have achieved results which are significantly better than those which have resulted from previous calculations. This approach can be extended (with some additional complexity) to the asymmetric NH_2D and ND_2H (*9*). It will be interesting to compare the results of a theoretical calculation of this nature and the experimental values reported in this paper.

Previous to this work, Weiss and Strandberg and Lichtenstein, Gallagher, and Derr (*10*) have studied the complex rotation–inversion spectrum of the partially deuterated species of this molecule and have assigned a number of transitions. However, they were unable to generally characterize the spectrum or to calculate the rotational constants. Such a characterization requires the measurement of a number of submillimeter wave transitions as well as the use of centrifugal distortion theory which has only recently been successfully applied to the study of light asymmetric rotors. The results of the present study also show that in the case of ND_2H it is necessary to include the effects of a vibration–rotation interaction which significantly alters the frequencies of a number of transitions.

In this paper we report the measurement of 82 new transitions which include many low J submillimeter lines. This data is then analyzed in order to obtain the rotation, distortion, inversion, and perturbation parameters of the partially deuterated ammonias.

EXPERIMENTAL

We have previously described a microwave spectrometer which makes possible measurements, accurately referenced to WWVB, of transitions to above 800 GHz and which is both convenient to use and reliable (*11*, *12*). These latter features are particularly important in the analysis of the spectrum of the partially deuterated ammonias because of the large number of measurements and long searches required in the data acquisition. This was particularly true in the early phases of the work before the spectrum was well characterized.

The sample used in this work was prepared by mixing NH_3 and D_2O in proportions such that equal numbers of hydrogen and deuterium nuclei were present. Since hydrogen and deuterium exchange rapidly in ammonia, the relative abundance of each isotopic species is determined statistically. As a result NH_3:NH_2D:ND_2H:ND_3 were present simultaneously in the absorption cell in the ratio 1:3:3:1. The ammonia was then removed by distillation. Small amounts of H_2O, HDO, and D_2O were also present and the stronger lines of these species were observable. These ex-

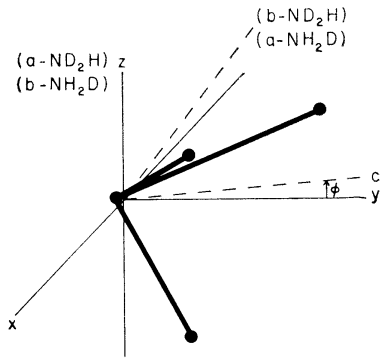

FIG. 1. Axis systems on the partially deuterated ammonias. The ϕ is positive for NH_2D and negative for ND_2H.

traneous lines provided no assignment problem because their spectra have been thoroughly characterized in the microwave region as the result of recent work (*13–15*).

SPECTRUM

NH_2D and ND_2H are light asymmetric rotors and, as such, have low-J rotational transitions scattered throughout the microwave region. Each of these transitions is split into a doublet by the inversion of molecular ammonia. The spectral analysis is complicated by the selection rules, which in addition to imposing the usual restrictions on asymmetric rotor transitions, also restrict the allowed transitions within, as well as between, the vibrational states. Figure 1 shows the relation of the molecular frame to both the *xyz* symmetry axis system and to the *abc* principal axis system. Since by symmetry the electric dipole moment lies along the *y* axis, which in both isotopes is rotated by only about 10° from the *c*-axis, *c*-type transitions will dominate the spectrum. However, NH_2D and ND_2H have small dipole moment components along the *a* and *b* axes, respectively, and as a consequence weaker *a*-type (NH_2D) and *b*-type (ND_2H) transitions are also observed.

The selection rules can be obtained from a consideration of the matrix elements of the electric dipole moment. The component of the electric dipole moment along a space fixed Z axis is

$$\mu_Z = \sum_g \Phi_{Zg}\mu_g,$$

where the μ_g are the components of the electric dipole moment along the principal axes of the moment of inertia tensor and where the Φ_{Zg} are the direction cosines. The matrix elements due to the component of the electric dipole moment along the g axis are

$$\langle J, K_{-1}, K_1, v|\mu_Z|J', K_{-1}', K_1', v'\rangle = \langle J, K_{-1}, K_1|\Phi_{Zg}|J', K_{-1}', K_1'\rangle\langle v|\mu_g|v'\rangle,$$

where J, K_{-1}, and K_1 specify the rotational state, and v specifies the vibrational state. $\langle J, K_{-1}, K_1|\Phi_{Zg}|J', K_{-1}', K'\rangle$ is simply related to the usual asymmetric rotor selection rules, while $\langle v|\mu_g|v'\rangle$ represents a restriction on transitions between vibrational levels. These restrictions can be determined from a consideration of the symmetry properties of the wave functions. In order that $\langle v|\mu_g|v'\rangle$ be nonzero, $\Psi^*_v\mu_g\Psi_{v'}$ must

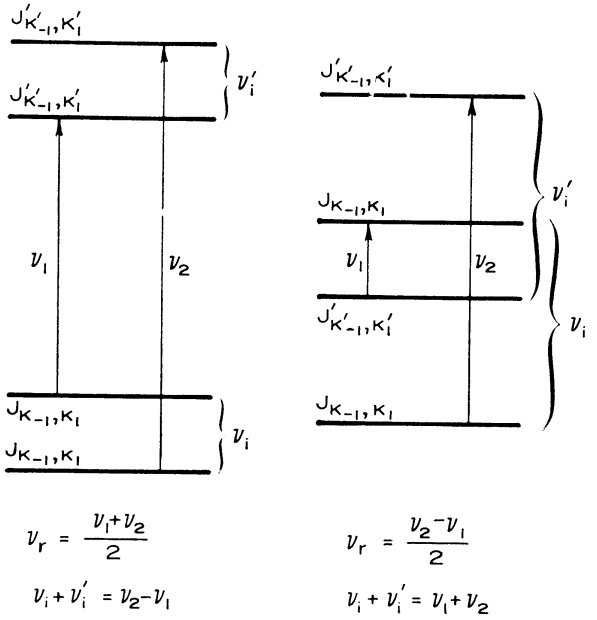

FIG. 2. Selection rules for c-type transitions (both NH_2D and ND_2H) for the case $\nu_r > \nu_i$ (left) and $\nu_r < \nu_i$ (right).

not change sign upon a reflection in a plane perpendicular to the inversion axis. For an inversion

$$\Psi_v' = (-1)^v \Psi_v.$$

Consequently, since μ_c changes sign during an inversion, allowed c-type transitions connect levels in adjacent vibrational states. On the other hand, a-type (NH_2D) and b-type (ND_2H) transitions connect levels within a given vibrational state since neither μ_a nor μ_b change sign during an inversion. These selection rules are illustrated in Figs. 2 and 3 (*6*).

INVERSION SPLITTING

The inversion splitting of ammonia as a function of both isotopic species and rotational state has been a subject of intensive study. It has been found that a function of the form (*16*)

$$\nu_i = \nu_0 \exp[a_1 J(J+1) + a_2 K^2 + a_3 J^2(J+1)^2 + a_4 J(J+1)K^2 + a_5 K^4 + \cdots] \quad (1)$$

will fit the observed inversion spectrum of NH_3 over a wide range of J, K states (*1*).

For the asymmetric forms of ammonia the direct inversion transitions are no longer allowed due to the lifting of the K degeneracy, but the frequency of this splitting can be deduced from the observed splitting of each rotation–inversion doublet. The analysis of the inversion spectrum is important both to characterize the molecular inversions as a function of rotational state and also because it is an important intermediate step in the rotational analysis which we will describe. Since K is not a good quantum number for an asymmetric rotor, the direct application of expressions of the form of Eq. (1) is precluded. In their early study of the partially deuterated am-

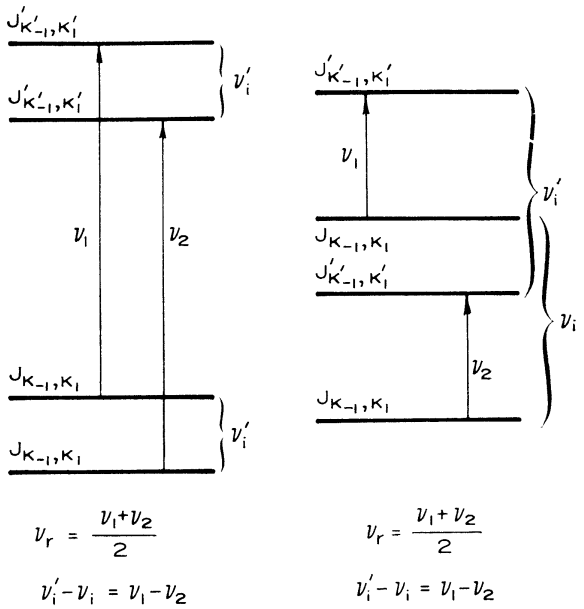

FIG. 3. Selection rules for a-type (NH_2D) and b-type (ND_2H) transitions for the case $\nu_r > \nu_i$ (left) and $\nu_r < \nu_i$ (right).

monias, Weiss and Strandberg suggested that since the c-axis (y axis in a prolate asymmetric rotor) nearly coincides with the geometric symmetry axis, $\langle P_y^{2n} \rangle$ be substituted for K^{2n} in the power series expansion. Several analyses based on this substitution have been performed, but they have been found to provide only general agreement even when applied to the rather limited data sets previously available (*10*). When formulations of this type are applied to the extensive data sets now available, severe discrepancies are encountered.

In retrospect, this is not surprising since this approach is analogous to fitting the rotational spectrum of an asymmetric rotor with only symmetric rotor distortion parameters. If, however, Eq. (1) is modified to include a complete set of angular momentum terms excellent results are obtained. A function of the form[3]

$$\nu_i = \nu_0 \exp[a_1 J(J+1) + a_2\langle P_y^2\rangle + a_3\langle P_z^2\rangle + a_4 J^2(J+1)^2 + a_5\langle P_y^2\rangle J(J+1) + a_6\langle P_z^2\rangle J(J+1) + a_7\langle P_y^4\rangle + a_8\langle P_y^2\rangle\langle P_z^2\rangle] \quad (2)$$

is found to fit a wide range of types of transitions and to accurately predict unobserved inversion frequencies. The angular momenta operators are evaluated in the rigid rotor basis.

HAMILTONIAN

Watson's formulation (*17*) of a reduced centrifugal distortion Hamiltonian has been used recently to analyze the rotational spectra of several light asymmetric rotors. The results of these analyses indicate that this model, when extended to high order,

[3] Because of the relation $P^2 = P_x^2 + P_y^2 + P_z^2$, inclusion of terms such as $a_i P_x^2$ would lead to fitting indeterminancies. $a_i P_z^4$ is not included for similar reasons.

introduces negligible model error (*18*). For NH_2D this Hamiltonian has the form

$$\mathcal{H} = \mathcal{H}_r + \mathcal{H}_d^{(4)} + \mathcal{H}_d^{(6)} + \mathcal{H}_d^{(8)}, \tag{3}$$

$$\mathcal{H}_r = \tfrac{1}{2}(\mathfrak{B} + \mathfrak{C})P^2 + [\mathfrak{A} - \tfrac{1}{2}(\mathfrak{B} + \mathfrak{C})](P_z^2 - b_p P_-^2), \tag{3a}$$

$$\mathcal{H}_d^{(4)} = -\Delta_J P^4 - \Delta_{JK} P^2 P_z^2 - \Delta_K P_z^4 - 2\delta_J P^2 P_-^2 - \delta_K (P_z^2 P_-^2 + P_-^2 P_z^2), \tag{3b}$$

$$\mathcal{H}_d^{(6)} = H_J P^6 + H_{JK} P^4 P_z^2 + H_{KJ} P^2 P_z^4 + H_K P_z^6 + 2h_J P^4 P_-^2 + h_{JK} P^2 (P_z^2 P_-^2 + P_-^2 P_z^2) + h_K (P_z^4 P_-^2 + P_-^2 P_z^4), \tag{3c}$$

$$\mathcal{H}_d^{(8)} = L_K P_z^8, \tag{3d}$$

where $P^2 = (P_x^2 + P_y^2 + P_z^2)$ is the total angular momentum, $P_-^2 = (P_x^2 - P_y^2)$, and $b_p = (\mathfrak{C} - \mathfrak{B})/(2\mathfrak{A} - \mathfrak{B} - \mathfrak{C})$ is Wang's asymmetry parameter appropriate for a near prolate top. The observed transitions of ND_2H do not require the $\mathcal{H}_d^{(8)}$ term. The terms in the Hamiltonian were chosen by means of a criteria which we have previously discussed (*19*).

It has been pointed out above that the spectrum of ND_2H is perturbed by the presence of a vibration–rotation interaction. Perturbations of this type have been considered by Lide (*20*) in the cyanamide molecule. When his results are specialized to ND_2H, the terms which couple adjacent vibrational states can be written

$$\mathcal{H}' = \mathcal{H}_1' + \mathcal{H}_2' = 2DP_y - i2E(P_xP_z + P_zP_x), \tag{4}$$

where the y-axis is perpendicular to the plane of reflection symmetry in ND_2H. The corresponding matrix elements in the oblate symmetric rotor representation are given by

$$\langle J, K, v | \mathcal{H}_1' | J, K+1, v' \rangle = D[(J-K)(J+K+1)]^{\frac{1}{2}}, \tag{5}$$

$$\langle J, K, v | \mathcal{H}_2' | J, K+1, v' \rangle = E(2K+1)[(J-K)(J+K+1)]^{\frac{1}{2}}, \tag{6}$$

where $(v - v')$ is odd and D and E are constants to be determined. The size of the perturbation produced by these terms depends on the energy difference of the coupled levels and thus is interdependent with the solution of the rest of the problem.

ANALYSIS

Because the strong c-type transitions are between different vibrational states and because the number of a-type (NH_2D) and b-type (ND_2H) transitions which were observed is small, it is not possible, even in the absence of the ND_2H perturbation, to use the observed transition frequencies to separately calculate the rotation–distortion constants of each of the two lowest vibrational states. In addition, the presence of the vibration–rotation interaction in ND_2H significantly complicates the analysis of this molecule since it is no longer possible to analyze each vibrational state separately. In the absence of a knowledge of the existence of the vibration–rotation interaction as well as in the absence of the weaker a-type and b-type transitions in the available data set, Weiss and Strandberg proposed that each rotation–vibration doublet of NH_2D and ND_2H be averaged to produce the "pure rotational frequency" and thereby eliminate the selection rule problem.

More recently, molecules such as cyanamide, trimethylene sulfide, and cyclopentene have been studied. These exhibit spectra similar to that of the partially deuterated ammonias except that in these molecules the transitions within a particular vibrational state are strong and numerous and that problems associated with centrifugal distortion are minimal. Millen, Topping, and Lide have used Lide's Hamiltonian and a perturbation technique based on the Van Vleck transformation in an analysis of cyanamide (*21*). Butcher and Costain (*22*) have applied Lide's Hamiltonian to cyclopentene by means of a perturbation technique in which the contributions which arise from the rotation–vibration coupling are evaluated by use of the asymmetric rigid rotor wavefunctions. Both of these techniques fit most of the observed transitions to within expected experimental uncertainty, but several lines at higher J deviate significantly beyond the expected experimental error in each case. Attanasio, Bauder, and Gunthard (*23*) have reanalyzed cyanamide by use of an exact infinite matrix diagonalization, but their deviation between calculated and observed spectra are also significantly larger than experimental uncertainty. They conclude that Lide's model is inadequate to describe the interaction. In their study of trimethylene sulfide, Harris, Harrington, Luntz and Gwinn (*24*) take perhaps the most straightforward approach and simply diagonalize a matrix which includes both vibrational states simultaneously. The resulting energy levels depend upon eight spectral constants: three lower state rotational constants (A_0, B_0, C_0), three upper state rotational constants (A_1, B_1, C_1), the vibrational splitting (Δ), and an interaction constant (F_{01}). These eight constants are then calculated by an iterative least squares procedure. The results of this analysis are again in excellent agreement at low J, but deviate beyond expected experimental uncertainty at higher J.

It would in principle be possible to use this latter technique, with the addition of centrifugal distortion terms, to analyze the partially deuterated ammonias. However, because of the large number of centrifugal distortion constants required to describe the spectrum of light asymmetric rotors (a total of 33 constants would be required for NH_2D) an alternative procedure was adopted. It has been found that Eq. (2) provides an accurate model for the analysis of the inversion splitting in the partially deuterated ammonias. The results of this analysis can be used to calculate the inversion splittings of each rotational state, and this information then can be used to calculate the energy level differences which would correspond to transitions within a given vibrational state, thus eliminating the selection rule problem. For NH_2D these calculated energy differences can be analyzed by means of techniques which we have previously discussed (*18*) in order to obtain the rotation–distortion parameters in each of the two lowest vibrational states.

The vibration–rotation interaction which exists in ND_2H significantly complicates the analysis of this molecule since it is no longer possible to analyze each vibrational state separately, since the contribution of the rotation–vibration interaction to the observed frequencies depends upon the vibrational splitting. In order to analyze this molecule, the following procedure was adopted. Since the perturbing matrix elements are off diagonal in K_1 by one, energy levels which are widely separated from their $K_1 \pm 1$ neighbors are not seriously perturbed. Consequently, to a good approximation transitions between levels of this type can be treated by use of the nondegenerate rotation–distortion analysis discussed above. A reasonably good estimate

TABLE I. Observed transitions of NH_2D (MHz)

Transition	Lower component			Upper component		
	Observed frequency	Calculated frequency	Difference	Observed frequency	Calculated frequency	Difference
$1_{0,1} \leftarrow 0_{0,0}$	332 781.89	332 782.23	-0.34	332 822.51	332 822.67	-0.16
$1_{1,1} \leftarrow 1_{0,1}$	85 926.2[a]	85 926.01	0.19	110 153.4[a]	110 153.64	-0.24
$1_{1,0} \leftarrow 0_{0,0}$	470 271.68	470 270.88	0.80	494 454.55	494 454.07	0.48
$3_{1,2} \leftarrow 2_{0,2}$	49 982.85[a]	49 982.39	0.46	74 155.73[a]	74 155.54	0.19
$3_{2,2} \leftarrow 3_{1,2}$	452 065.61	452 065.92	-0.31	475 890.26	475 890.19	0.07
$2_{2,1} \leftarrow 2_{1,1}$	282 112.60	282 113.30	-0.70	305 723.67	305 724.19	-0.53
$2_{0,2} \leftarrow 1_{1,0}$	488 324.19	488 323.92	0.27	512 426.55	512 427.46	-0.91
$3_{1,3} \leftarrow 3_{0,3}$	18 807.74[a]	18 807.88	-0.14	43 042.16[a]	43 042.72	-0.56
$3_{1,2} \leftarrow 2_{2,1}$	451 752.64	451 753.30	-0.66	475 577.53	475 576.70	0.83
$3_{2,2} \leftarrow 4_{1,3}$	143 520.0[a]	143 520.31	-0.31	143 551.1[a]	143 550.92	0.18
$4_{3,2} \leftarrow 4_{2,2}$	472 707.14	472 706.53	0.61	494 928.66	494 929.50	-0.84
$4_{2,3} \leftarrow 5_{2,4}$	338 270.14	338 270.71	-0.57	338 932.83	338 932.38	0.45
$4_{1,3} \leftarrow 5_{0,5}$	7 562.06[a]	7 561.93	0.13	17 052.74[a]	17 052.62	0.12
$5_{2,4} \leftarrow 5_{1,4}$	76 398.6[a]	76 398.08	-0.48	99 118.6[a]	99 119.27	-0.67
$5_{3,3} \leftarrow 5_{2,3}$	375 079.09	375 079.16	-0.07	396 688.15	396 682.75	0.17
$6_{1,6} \leftarrow 6_{0,6}$	10 342.62[a]	10 342.64	-0.02	14 104.32[a]	14 104.14	0.18
$6_{3,4} \leftarrow 6_{2,4}$	265 814.19	265 814.24	-0.05	288 607.17	288 607.31	0.14
$7_{3,4} \leftarrow 7_{3,5}$	340 335.38	340 334.51	0.87	341 120.63	341 121.41	-0.78
$7_{3,5} \leftarrow 7_{2,5}$	102 621.7[a]	102 622.19	-0.49	102 104.2[a]	102 104.78	-0.58
$8_{1,8} \leftarrow 8_{0,8}$	12 764.10[a]	12 764.31	-0.21	15 115.94[a]	15 115.73	0.21
$8_{3,6} \leftarrow 8_{2,6}$	83 040.4[a]	83 040.50	-0.10	103 150.4[a]	103 150.24	0.16
$8_{4,5} \leftarrow 8_{3,5}$	417 053.81	417 054.51	-0.70	434 641.11	434 641.34	0.17
$9_{1,9} \leftarrow 9_{0,9}$	13 217.75[a]	13 217.93	-0.18	15 320.16[a]	15 320.24	0.20
$9_{4,6} \leftarrow 9_{3,6}$	278 604.59	278 604.18	0.40	294 424.50	294 424.80	-0.30
$10_{4,7} \leftarrow 10_{3,7}$	161 031.7[a]	161 030.69	1.01	178 232.6[a]	178 233.41	-0.81
$11_{3,7} \leftarrow 11_{4,7}$	424 050.33	424 050.05	-0.25	438 894.52	438 894.21	0.31
$12_{3,9} \leftarrow 12_{4,8}$	267 642.78	267 642.24	0.54	281 748.07	281 748.62	-0.55
$13_{3,10} \leftarrow 13_{4,9}$	147 371.00	147 371.55	-0.55	160 480.34	160 480.49	0.17

[a] Ref. 19.

of the size of the perturbation can be obtained from a comparison between the observed frequencies of the perturbed transitions and predictions of these frequencies based on the analysis of the unperturbed transitions.

It is found that the contributions of vibration–rotation interaction to the observed transition frequencies can be accurately evaluated in a matrix which contains only rigid rotor and inversion terms. This step is in fact equivalent to the technique of Ref. (*24*), but since the effects of centrifugal distortion are extremely large for

Table [illegible]. Observed Transitions of [illegible]

Transition	Lower Component: Observed frequency	Perturbation contribution	Unperturbed frequency	Calculated frequency	Difference	Upper Component: Observed frequency	Perturbation contribution	Unperturbed frequency	Calculated frequency	Difference
$[illegible]_{1,0} \leftarrow [illegible]_{0,1}$	[illegible]	[illegible]	110 810.81	110 812.34	0.51	[illegible]	2.40	[illegible]	[illegible]	[illegible]
$[illegible]_{1,1} \leftarrow 0_{0,0}$	[illegible]	-2.[illegible]	[illegible]	335 446.53	0.00	[illegible]	[illegible]	[illegible]	[illegible]	[illegible]
[illegible]	[illegible][a]	[illegible]	[illegible]	[illegible] 374.78	-0.[illegible]	[illegible][a]	[illegible]	[illegible]	[illegible]	[illegible]
[illegible]	[illegible]	[illegible]	[illegible]	[illegible] 500.74	-0.[illegible]	[illegible]	[illegible]	[illegible]	[illegible]	[illegible]
[illegible]	[illegible]	[illegible]	177 [illegible]	177 819.04	0.[illegible]	177 [illegible]	[illegible]	[illegible]	[illegible]	[illegible]
[illegible]	332 1[illegible]0.51	-2[illegible]	332 217.44	332 180.82	-0.31	332 445.[illegible]	-1[illegible]	[illegible]	[illegible]	[illegible]
[illegible]	[illegible]	[illegible]	[illegible]	206 972.42	-0.56	207 170.50	2[illegible]	[illegible]	[illegible]	[illegible]
[illegible]	[illegible]	1.[illegible]	463 626.70	463 628.33	0.26	463 [illegible]	2.34	463 [illegible]	[illegible]	[illegible]
[illegible]	[illegible] 560.[illegible][a]	-0.[illegible]	28 561.54	28 561.83	-0.93	33 739.13[a]	-0.[illegible]	33 739.[illegible]	[illegible]	[illegible]
[illegible]	[illegible]	2[illegible].47	346 324.[illegible]	346 353.47	-0.04	35[illegible] 22[illegible].21	17.21	[illegible]	[illegible]	[illegible]
[illegible]	183 188.35	-17.15	183 205.48	183 188.51	-0.18	193 007.70	-28.42	[illegible]	[illegible]	[illegible]
[illegible]	410 490.71	-2.00	410 492.71	410 490.77	-0.06	420 634.35	-2.46	420 636.81	[illegible]	[illegible]
[illegible]	296 477.08	0.51	296 476.57	296 477.31	-0.23	[illegible]	0.52	[illegible]	[illegible]	[illegible]
[illegible]	[illegible]	3.70	[illegible]	212 246.67	0.20	212 411.44	4.17	[illegible]	[illegible]	[illegible]
[illegible]	8 [illegible][a]	-0.23	8 284.15	8 283.96	-0.04	15 481.[illegible][a]	-0.25	[illegible]	[illegible]	[illegible]
[illegible]	126 5[illegible]	-4.27	126 601.66	126 597.20	0.19	136 382.41	-4.76	136 387.17	[illegible]	[illegible]
$[illegible]_{2,3} \leftarrow [illegible]_{1,3}$	268 027.20	1.40	268 025.80	268 026.23	0.97	268 174.04	1.47	[illegible]	[illegible]	[illegible]
$4_{[illegible]} \leftarrow 4_{1,3}$	69 581.[illegible][a]	-1.52	69 583.12	69 580.88	0.72	[illegible] 302.[illegible][a]	-1.[illegible]	[illegible] 304.40	[illegible] 302.[illegible]	[illegible]
[illegible]	257 4[illegible].75	-24.[illegible]	[illegible]	257 404.26	0.49	[illegible]	-31.[illegible]	[illegible]	[illegible]	-0.31
[illegible]	383 352.88	0.84	383 352.04	383 352.81	0.07	383 503.40	[illegible]	[illegible]	[illegible]	[illegible]
[illegible]	309 716.30	5.76	309 710.54	309 716.43	-0.13	309 [illegible]	[illegible]	[illegible]	[illegible]	[illegible]
[illegible]	28 677.80[a]	-0.[illegible]	28 678.45	28 678.12	-0.26	35 320.[illegible][a]	[illegible]	[illegible]	[illegible]	-0.47
[illegible]	201 [illegible].75	-[illegible].08	201 [illegible]	201 [illegible]	0.[illegible]	211 050.[illegible]	-7.75	[illegible]	211 05[illegible].81	-0.0[illegible]
[illegible]	4 [illegible].20[a]	[illegible]	4 [illegible].20	4 [illegible]	-0.10	[illegible]	[illegible]	[illegible]	[illegible]	[illegible]
[illegible]	[illegible] 301.[illegible][a]	-0.[illegible]	[illegible]	7 301.[illegible]	-0.11	[illegible][a]	[illegible]	[illegible]	[illegible]	-0.14
[illegible]	[illegible][a]	[illegible]	[illegible]	[illegible]	[illegible]	[illegible]	[illegible]	[illegible]	[illegible]	[illegible]
[illegible]	[illegible]	[illegible]	[illegible]	[illegible]	[illegible]	[illegible]	[illegible]	[illegible]	[illegible]	[illegible]
[illegible]	[illegible]	[illegible]	[illegible]	[illegible]	[illegible]	[illegible]	[illegible]	[illegible]	[illegible]	[illegible]
[illegible]	[illegible]	-10.[illegible]	[illegible]	[illegible]	-0.30	[illegible]	-11.[illegible]	[illegible]	[illegible]	[illegible]
$[illegible] \leftarrow [illegible]_{0,[illegible]}$	5 364.03[a]	0.00	5 364.03	5 363.97	0.06	[illegible] 414.1[illegible][a]	0.00	[illegible]	[illegible]	[illegible]
[illegible]	20 608.77[a]	-0.[illegible]	20 609.[illegible]	20 608.05	-0.[illegible]	[illegible] 31[illegible].47[a]	-0.46	[illegible]	[illegible]	-0.14
[illegible]	[illegible]	-4.0[illegible]	175 [illegible]	175 855.34	0.41	[illegible]	-4.[illegible]	[illegible]	[illegible]	[illegible]
[illegible]	[illegible]	[illegible]	[illegible]	[illegible]	0.10	[illegible] 087.15	[illegible]	[illegible]	[illegible]	[illegible]
[illegible]	[illegible][a]	[illegible]	5 4[illegible]	[illegible]	[illegible]	[illegible][a]	[illegible]	[illegible]	[illegible]	[illegible]
[illegible]	[illegible][a]	[illegible]	[illegible]	[illegible] 488.14	[illegible]	[illegible] 361.2[a]	[illegible]	[illegible]	[illegible]	[illegible]
[illegible]	[illegible]	[illegible]	[illegible]	[illegible]	[illegible]	[illegible]	[illegible]	[illegible]	[illegible]	[illegible]
$[illegible] \leftarrow [illegible]_{[illegible],10}$	[illegible][a]	[illegible]	[illegible]	[illegible]	[illegible]	[illegible][a]	[illegible]	[illegible]	[illegible]	[illegible]
[illegible]	[illegible]	[illegible]	[illegible]	[illegible]	[illegible]	[illegible]	[illegible]	[illegible]	[illegible]	[illegible]
$[illegible]_{[illegible],11} \leftarrow [illegible]_{[illegible],11}$	[illegible][a]	[illegible]	[illegible]	[illegible]	[illegible]	[illegible][a]	[illegible]	[illegible]	[illegible]	[illegible]
[illegible]	[illegible]	[illegible]	133 337.40	133 338.02	[illegible]	[illegible]	[illegible]	[illegible]	[illegible]	[illegible]
$11_{[illegible],6} \leftarrow 11_{[illegible]}$	473 [illegible].35	-20.[illegible]	473 [illegible]	473 [illegible].75	0.[illegible]	4[illegible]0 221.3[illegible]	-21.1[illegible]	[illegible]	4[illegible]0 221.[illegible]	-0.47
$12_{[illegible],7} \leftarrow 12_{[illegible],7}$	318 728.3[illegible]	-[illegible].05	318 736.41	318 728.41	-0.0[illegible]	324 77[illegible].40	-[illegible]	324 787.[illegible]	324 [illegible].18	0.21
$13_{[illegible]} \leftarrow 13_{[illegible]}$	185 718.28	-[illegible]	185 721.[illegible]	185 718.24	0.04	[illegible] 424.[illegible]	-[illegible]	[illegible]	[illegible]	0.14

[a] [illegible]

Table III. NH_2D inversion splitting analysis (MHz)

Transition	Observed frequency	Calculated frequency	Difference
$^{1}_{0,1} \leftarrow {}^{0}_{0,0}$	40.62	40.44	0.18
$^{1}_{1,1} \leftarrow {}^{1}_{0,1}$	24 227.20	24 227.62	-0.42
$^{1}_{1,0} \leftarrow {}^{0}_{0,0}$	24 182.87	24 183.19	-0.32
$^{2}_{1,2} \leftarrow {}^{2}_{0,2}$	24 182.88	24 183.15	-0.27
$^{2}_{2,0} \leftarrow {}^{2}_{1,2}$	23 824.65	23 824.26	0.39
$^{3}_{2,1} \leftarrow {}^{3}_{1,1}$	23 611.07	23 610.89	0.18
$^{2}_{0,2} \leftarrow {}^{1}_{1,0}$	24 102.36	24 103.54	-1.18
$^{3}_{1,2} \leftarrow {}^{2}_{0,2}$	24 234.74	24 234.83	-0.09
$^{3}_{1,3} \leftarrow {}^{2}_{2,1}$	23 394.43	23 393.34	1.09
$^{2}_{2,3} \leftarrow {}^{1}_{1,2}$	22 961.10	22 960.01	1.09
$^{3}_{2,2} \leftarrow {}^{3}_{2,3}$	22 221.52	22 222.87	-1.35
$^{4}_{3,2} \leftarrow {}^{3}_{3,1}$	662.68	661.67	1.02
$^{4}_{1,3} \leftarrow {}^{3}_{0,3}$	24 614.50	24 614.75	0.06
$^{3}_{3,1} \leftarrow {}^{3}_{2,1}$	22 720.00	22 720.19	-0.19
$^{4}_{3,2} \leftarrow {}^{4}_{2,3}$	21 604.10	21 603.56	0.54
$^{4}_{1,3} \leftarrow {}^{4}_{0,4}$	21 944.54	21 944.77	0.17
$^{5}_{3,2} \leftarrow {}^{5}_{2,4}$	20 393.31	20 393.40	0.91
$^{7}_{3,4} \leftarrow {}^{7}_{2,5}$	735.30	736.80	-1.50
$^{7}_{3,5} \leftarrow {}^{7}_{2,6}$	20 452.30	20 452.56	-0.26
$^{4}_{1,3} \leftarrow {}^{4}_{0,4}$	25 204.04	25 203.95	0.09
$^{5}_{3,2} \leftarrow {}^{5}_{2,4}$	20 129.00	20 127.83	1.17
$^{6}_{3,3} \leftarrow {}^{6}_{2,5}$	19 807.80	19 806.74	0.96
$^{5}_{1,4} \leftarrow {}^{5}_{0,5}$	24 635.24	24 635.20	0.04
$^{6}_{1,5} \leftarrow {}^{6}_{0,6}$	17 770.06	17 770.76	-0.70
$^{10}_{4,7} \leftarrow {}^{10}_{3,7}$	17 300.90	17 302.72	-1.82
$^{11}_{5,7} \leftarrow {}^{11}_{4,7}$	14 524.69	14 524.15	0.54
$^{12}_{5,8} \leftarrow {}^{12}_{4,8}$	14 105.29	14 106.38	-1.09
$^{13}_{5,9} \leftarrow {}^{13}_{4,9}$	13 808.06	13 806.95	1.01

light asymmetric rotors, it must be used as an intermediate step before a rotation–distortion analysis. Furthermore, since these contributions are relatively insensitive to the exact size of the other terms, the perturbations, once calculated, remain relatively constant as small changes are made in either the rotational or inversion analyses. Thus, the perturbations calculated by this technique can be subtracted from the observed frequencies to produce "unperturbed" frequencies which can be analyzed in the usual nondegenerate manner. In practice the perturbation constant D is adjusted to produce the minimum rms deviation in the rotation–distortion analysis. A number of iterations of this procedure are required in order to optimize the fit.

Table IV. NH_2H inversion splitting analysis (MHz)

Transition	Observed splitting	Perturbation contribution	Unperturbed splitting	Calculated splitting	Difference
$1_{1,0} \leftarrow 1_{0,1}$	53.46	0.46	53.92	53.91	0.04
$1_{1,1} \leftarrow 0_{0,0}$	67.48	0.46	67.02	67.49	-0.01
$1_{1,1} \leftarrow 1_{0,1}$	10 166.76	-0.46	10 167.22	10 167.15	-0.39
$1_{1,0} \leftarrow 0_{0,0}$	10 151.50	-0.46	10 151.96	10 150.54	0.96
$2_{1,1} \leftarrow 2_{0,2}$	101.38	0.05	101.43	101.09	-0.11
$2_{2,1} \leftarrow 2_{1,2}$	255.42	11.17	244.25	254.91	0.51
$2_{2,0} \leftarrow 2_{1,1}$	198.64	11.17	187.47	198.33	0.31
$2_{0,2} \leftarrow 1_{1,1}$	59.90	0.44	59.45	60.29	-0.39
$2_{1,2} \leftarrow 2_{0,2}$	10 178.23	-0.05	10 178.28	10 176.48	1.75
$2_{3,0} \leftarrow 2_{1,2}$	9 875.78	-11.26	9 887.04	9 876.17	-0.39
$2_{2,1} \leftarrow 2_{1,1}$	9 819.46	-11.26	9 830.72	9 819.58	-0.12
$2_{0,2} \leftarrow 1_{1,0}$	10 143.61	-0.44	10 144.10	10 143.53	0.01
$3_{1,2} \leftarrow 3_{0,3}$	138.62	0.01	138.61	138.74	0.08
$3_{2,1} \leftarrow 3_{1,2}$	164.57	0.46	164.11	164.88	-0.31
$3_{1,3} \leftarrow 3_{0,3}$	10 197.99	-0.02	10 198.01	10 197.75	0.24
$3_{2,2} \leftarrow 3_{1,2}$	9 785.02	-0.49	9 785.51	9 785.17	-0.15
$4_{2,2} \leftarrow 4_{1,3}$	146.84	0.07	146.77	147.76	-0.92
$4_{2,3} \leftarrow 4_{1,3}$	9 721.20	-0.09	9 721.29	9 721.91	-0.71
$4_{3,2} \leftarrow 4_{2,2}$	9 223.58	-7.35	9 230.93	9 224.38	-0.80
$5_{2,3} \leftarrow 5_{1,4}$	150.61	0.02	150.60	150.89	-0.28
$5_{3,2} \leftarrow 5_{2,3}$	245.21	0.59	245.32	246.80	-0.39

RESULTS

The observed transitions of NH_2D and ND_2H are shown in Tables I and II, respectively. As in the case of other light asymmetric rotors, it is the low J transitions which are of primary importance in that they primarily determine the rotational constants and P^4 distortion terms. Inspection of these tables indicates that many of these transitions fall in the submillimeter region of the spectrum. On the other hand, the Q-branch series which tend toward zero frequency with increasing J contain little independent information at higher J. Also included in Table II is the contribution of the rotation–vibration interaction to the observed frequency and the "unperturbed" frequency which is calculated by the removal of this contribution. The results of the inversion analyses, which are necessary to convert observed transition frequencies to energy level differences within a given vibrational state, are shown in Tables III and IV. The inversion constants which result from these analyses are shown in Table V. These energy level differences were then analyzed and the resulting rotation–distortion constants for the 0^+ and 0^- states shown in Table VI. The number of places retained in these constants is dictated by the number of places required to reproduce the calculated spectrum to within experimental uncertainty. Because of the

Table IV. (Continued)

Transition	Observed splitting	Perturbation contribution	Unperturbed splitting	Calculated splitting	Difference
$9_{2,7} \leftarrow 9_{1,8}$	9 [illegible]	-0.04	[illegible]	[illegible]	-0.31
$7_{3,5} \leftarrow 7_{2,6}$	[illegible]	-0.[illegible]	[illegible]	9 145.28	-0.31
$7_{1,6} \leftarrow 7_{0,7}$	10 141.28	-0.01	10 141.29	10 141.11	-0.18
$6_{2,5} \leftarrow 6_{1,6}$	9 [illegible]	-0.02	[illegible]	[illegible]	0.03
$5_{3,3} \leftarrow 5_{2,4}$	[illegible]	-0.[illegible]	[illegible]	7 020.70	-1.30
$8_{4,5} \leftarrow 8_{3,6}$	[illegible]	-7.32	[illegible]	[illegible]	0.00
$7_{6,2} \leftarrow 7_{5,3}$	327.10	0.07	326.13	327.54	-0.44
$7_{4,4} \leftarrow 7_{3,5}$	[illegible]	-0.[illegible]	[illegible]	301.32	0.35
$8_{1,8} \leftarrow 8_{0,8}$	10 77[illegible]	0.00	10 77[illegible]	10 775.03	0.[illegible]
$8_{3,6} \leftarrow 8_{2,6}$	[illegible]	-0.03	[illegible]	[illegible]	0.13
$8_{4,5} \leftarrow 8_{3,5}$	[illegible]	-0.14	8 135.36	8 132.17	-0.33
$8_{5,4} \leftarrow 8_{4,4}$	7 435.14	-7.[illegible]	7 43[illegible]	7 435.[illegible]	-0.[illegible]
$11_{1,9} \leftarrow 11_{0,9}$	11 002.73	0.00	11 002.73	11 002.53	0.20
$11_{4,8} \leftarrow 11_{3,8}$	7 [illegible]	-0.04	7 [illegible]	7 [illegible]	-0.37
$11_{5,7} \leftarrow 11_{4,7}$	7 [illegible]	-0.[illegible]	7 [illegible]	7 [illegible]	1.12
$10_{1,10} \leftarrow 10_{0,10}$	11 [illegible]	0.00	11[illegible]	11 [illegible]	0.[illegible]
$10_{5,6} \leftarrow 10_{4,6}$	7 121.[illegible]	-0.17	7 122.03	7 120.[illegible]	0.[illegible]
$11_{1,11} \leftarrow 11_{0,11}$	11 [illegible]	0.00	11 [illegible]	11 [illegible]	-0.22
$11_{5,7} \leftarrow 11_{4,7}$	[illegible]	-0.04	[illegible]	[illegible]	0.38
$11_{6,6} \leftarrow 11_{5,6}$	[illegible]	-0.[illegible]	6 214.02	6 211.12	-1.04
$12_{6,7} \leftarrow 12_{5,7}$	[illegible]	-0.[illegible]	[illegible]	7 050.78	0.26
$12_{6,6} \leftarrow 12_{5,8}$	[illegible]	-0.04	[illegible]	[illegible]	-0.18

high correlation among the higher order constants, this number can differ significantly from that indicated by the size of the uncertainty. These constants and the inversion constants (and for ND_2H, the perturbation constant) were then used to calculate a theoretical spectrum. Comparisons of these calculated frequencies with the observed frequencies are shown in Tables I and II. It was found that the interaction constant E is perfectly correlated with the rotation–distortion constants and consequently with D fixed widely varying values of E produced the same fit. E was therefore fixed at zero.

DISCUSSION

Of primary importance is a determination of whether or not significant model errors exist at any point in the analysis. It should be noted that for both NH_2D and ND_2H the rms deviation of the rotation–distortion analysis is approximately $\frac{1}{2}$ the rms deviation of the inversion fit. This is to be expected if experimental uncertainty dominates model error. The rotation–distortion analysis effectively averages the frequency of each observed doublet and then adds or subtracts a theoretically gen-

TABLE V. Inversion constants of partially deuterated ammonia (MHz)

	NH_2D		ND_2H	
	Constant	σ	Constant	σ
ν_0	12 150.68	0.36	5 113.48	0.15
a_1	(-5.142)	$0.003)\times10^{-3}$	(-2.0693	$0.004)\times10^{-3}$
a_2	(7.0656	$0.301)\times10^{-3}$	(3.7316	$0.005)\times10^{-3}$
a_3	(-2.5764	$0.014)\times10^{-3}$	(-1.3472	$0.002)\times10^{-2}$
a_4	(-3.15	$0.18)\times10^{-6}$	(-3.9	$1.2)\times10^{-7}$
a_5	(3.43	$0.3)\times10^{-6}$	(1.460	$0.07)\times10^{-5}$
a_6	(1.50	$0.11)\times10^{-5}$	(-2.43	$0.7)\times10^{-6}$
a_7	(-5.45	$0.4)\times10^{-6}$	(-1.573	$0.06)\times10^{-5}$
a_8	(-3.04	$0.1)\times10^{-5}$	(-5.28	$0.3)\times10^{-5}$

erated inversion correction. The net result of this procedure would be to approximately decrease the contribution of experimental error to the rms deviation by $\sqrt{2}$. On the other hand, each inversion splitting results from subtracting two observed frequencies. The net result of this procedure would be to approximately increase the contribution of experimental error to the rms deviation by $\sqrt{2}$. Since the rms deviations do differ by approximately this factor of 2, it can be inferred that experimental error is the predominant contribution to the rms deviations and that model errors are minimal. While the rms deviations are somewhat larger than would be expected from the experimental data newly reported here, they are consistent with the data set taken as a whole. The larger deviation in NH_2D may be inherent in the data set or due to a small-vibration rotation interaction. Since the ND_2H data in fact fits better than the NH_2D, it can also be inferred that the rotation–vibration interaction has been accurately accounted for. Since the deviations observed for both isotopes of ammonia are not only consistent with experimental error but also smaller in an absolute sense than the deviations encountered in the analyses of the heavier molecules discussed above, it would not be unreasonable to assume that the inclusion of centrifugal distortion effects in these analyses would significantly improve the fits.

At present the major problem associated with the application of the Watson Hamiltonian to the lightest asymmetric rotors is its slow convergence both in terms of the number of constants required to adequately fit observed transitions and the related difficulty of predicting accurately transitions at J higher than included in the data set. These problems are most evident in light planar asymmetric rotors such as HDO and D_2S. In these cases it is difficult to predict transitions at the next higher J. In addition, Hamiltonians with more than 20 terms are barely adequate to describe the data set. Carpenter (*25*) has recently suggested that choice of molecular z-axis can affect this convergence and has demonstrated the effect for the relatively heavy molecules carbonyl fluoride and sulfur dioxide. It will be interesting to see if more advantageous axis selection can be made for the light asymmetric rotors and if such a selection significantly improves the situation. Major efforts are also underway to construct Hamiltonians which take into account the geometry of XYZ

TABLE VI. Rotation and distortion parameters of partially deuterated ammonia (MHz)[a]

	NH_2D				ND_2H			
	0^+		0^-		0^+		0^-	
	Constant	σ	Constant	σ	Constant	σ	Constant	σ
A	230 286.53	0.21	230 192.14	0.21	223 222.92	0.18	223 147.21	0.14
B	192 240.15	0.42	192 176.27	0.42	160 433.96	0.17	160 423.37	0.13
C	140 802.80	0.42	140 828.74	0.42	112 305.40	0.17	112 315.72	0.13
Δ_J	4.4437	0.010	4.4231	0.010	4.051	0.02	4.075	0.02
Δ_{JK}	9.57553	0.042	9.30020	0.042	-6.11325	0.04	-6.03053	0.03
Δ_K	4.7525	0.053	4.8465	0.052	22.1420	0.04	21.4455	0.03
δ_J	1.07491	0.011	1.05245	0.011	1.16538	0.0015	1.16439	0.0012
δ_K	14.674	0.23	14.140	0.24	4.6171	0.013	4.5235	0.015
Φ_J	0.04540540	0.014	0.04278492	0.011	0.0134406	0.004	0.0124765	0.005
Φ_{JK}	-0.12[illegible]60	0.03[illegible]	-0.11[illegible]117	0.03[illegible]	-0.0440645	0.009	-0.0333341	0.007
Φ_K	0.11447	0.031	0.10577	0.030	0.043361	0.006	0.031281	0.005
ϕ_J	0.00143[illegible]7	0.00041	0.0012134	0.00046	0.000[illegible]6877	0.0002	0.0007[illegible]360	0.0002
ϕ_{JK}	-0.017[illegible]7	0.0072	-0.01553	0.0071	-0.010521	0.002	-0.007320[illegible]	0.002
ϕ_K	0.10341	0.032	0.09[illegible]49	0.031	0.028025	0.005	0.022[illegible]07	0.004
L_{JK}	-0.0001854	0.000059	-0.0001044	0.00003[illegible]				
L						0.002[illegible]4	0.0001	
κ	-0.31004[illegible]		-0.310[illegible]9[illegible]		-0.132174		-0.131887	
rms	0.42		0.41		0.34		0.26	

a. The number of digits retained in the spectroscopic constants are determined by the requirement that the constants reproduce the spectra to within experimental error. See text.

molecules in hopes of solving some of these problems for this particular class of molecule (*8*, *26*). These interesting efforts have not as yet resulted in models of sufficient accuracy for the analysis of high resolution microwave data, but it is reasonable to assume their ultimate success. Similar approaches for more complicated molecules are certain to be even more complicated and difficult. It would therefore be particularly useful if use of the present power series Hamiltonians did not result in these convergence problems for the nonplanar light asymmetric rotors. The analyses of the partially deuterated ammonias indicate that this is the case. Not only can the observed transitions be accurately fit and unmeasured transition within the general range of the data set be accurately predicted (this is also true for the XY_2 and XYZ molecules studied) (*18*), but it is also possible to accurately predict transitions at J's significantly higher than the J's included in the analysis. Furthermore, both NH_2D and ND_2H require significantly fewer distortion constants than the planar molecules which have been previously investigated.

ACKNOWLEDGMENTS

We express our appreciation to Walter Gordy for his support during this work. Some of the programs used in this work were developed and written by Robert L. Cook. One of us (P.H.) acknowledges support from a grant to the Department of Physics, Duke University by the Shell Companies Foundation.

RECEIVED: May 9, 1974

REFERENCES

1. E. SCHNABEL, T. TORRING, AND W. WILKE, *Z. Physik* **188**, 167 (1965).
2. G. HERMANN, *J. Chem. Phys.* **29**, 875 (1958).
3. P. HELMINGER, F. C. DE LUCIA, AND W. GORDY, *J. Mol. Spectrosc.* **39**, 94 (1971).

4. P. HELMINGER, F. C. DE LUCIA, W. GORDY, H. W. MORGAN, and P. A. STAATS, *Phys. Rev. A* **9**, 12 (1974).
5. R. L. COOK, G. E. JONES, F. C. DE LUCIA, AND P. HELMINGER, Abstract B3, Symposium on Molecular Structure and Spectroscopy, Columbus, Ohio, 1973.
6. J. E. WOLLRAB, "Rotational Spectra and Molecular Structure," Academic Press, New York 1967.
7. D. PAPOUSEK, J. M. R. STONE, AND V. SPIRKO, *J. Mol. Spectrosc.* **48**, 17 (1973).
8. J. T. HOUGEN, P. R. BUNKER, AND J. W. C. JOHNS, *J. Mol. Spectrosc.* **34**, 136 (1970).
9. V. DANIELS, D. PAPOUSEK, V. SPIRKO, AND M. HORAK, *J. Mol. Spectrosc.*, submitted for publication.
10. M. T. WEISS AND M. W. P. STRANDBERG, *Phys. Rev.* **83**, 567 (1951); M. LICHTENSTEIN, J. J. GALLAGHER, AND V. E. DERR, *J. Mol. Spectrosc.* **12**, 87 (1964).
11. P. HELMINGER, F. C. DE LUCIA, AND W. GORDY, *Phys. Rev. Lett.* **25**, 1397 (1970).
12. P. HELMINGER, R. L. COOK, AND F. C. DE LUCIA, *J. Mol. Spectrosc.* **40**, 125 (1971).
13. F. C. DE LUCIA, P. HELMINGER, R. L. COOK, AND W. GORDY, *Phys. Rev. A* **5**, 487 (1972).
14. F. C. DE LUCIA, R. L. COOK, P. HELMINGER, AND W. GORDY, *J. Chem. Phys.* **55**, 5334 (1971).
15. W. S. BENEDICT, S. A. CLOUGH, L. FRENKEL, AND T. E. SULLIVAN, *J. Chem. Phys.* **53**, 2565 (1970).
16. C. C. COSTAIN, *Phys. Rev.* **82**, 108 (1951).
17. J. K. G. WATSON, *J. Chem. Phys.* **45**, 1360 (1966); **46**, 1935 (1967); **48**, 4517 (1968).
18. F. C. DE LUCIA, P. HELMINGER, W. GORDY, H. W. MORGAN, AND P. A. STAATS, *Phys. Rev. A* **8**, 2785 (1973). See also Refs. (*12–14*, *19*).
19. R. L. COOK, F. C. DE LUCIA, AND P. HELMINGER, *J. Mol. Spectrosc.* **41**, 123 (1972).
20. D. R. LIDE, JR., *J. Mol. Spectrosc.* **8**, 142 (1962).
21. D. J. MILLEN, G. TOPPING, AND D. R. LIDE, *J. Mol. Spectrosc.* **8**, 153 (1962).
22. S. S. BUTCHER AND C. C. COSTAIN, *J. Mol. Spectrosc.* **15**, 40 (1965).
23. A. ATTANASIO, A. BAUDER, AND HS. H. GUNTHARD, *Mol. Phys.* **24**, 889 (1972).
24. D. O. HARRIS, H. W. HARRINGTON, A. C. LUNTZ, AND W. D. GWINN, *J. Chem. Phys.* **44**, 3467 (1966).
25. J. H. CARPENTER, *J. Mol. Spectrosc.* **46**, 348 (1973).
26. A. R. HOY AND P. R. BUNKER, *J. Mol. Spectrosc.* **52**, 439 (1974).